

## Exploring runoff processes using chemical, isotopic and hydrometric data in a discontinuous permafrost catchment

Jessica L. Boucher and Sean K. Carey

### ABSTRACT

Hydrometric, isotopic and hydrochemical data were used to investigate runoff generation in a discontinuous permafrost headwater catchment. Research was undertaken between 10 April and 8 July 2008 within Granger Basin, a 7.6 km<sup>2</sup> sub-catchment of the Wolf Creek Research Basin, Yukon Territory, Canada. The objectives of this research were to utilize hydrometric, stable isotope and hydrochemical methods to: (i) establish water balance components and (ii) couple water balance information with stable isotope and hydrochemical information to provide an enhanced understanding of runoff sources and pathways. The water balance components were snowmelt (152 mm), precipitation (68 mm), evaporation (88 mm), discharge (173 mm) and change in storage (–41 mm). The runoff ratio was high compared with previous years in this catchment. Using two-component hydrograph separation, pre-event water represented ~73% of total discharge during freshet. End-member mixing diagrams suggested three contributing sources to streamflow in the following order: groundwater, soil water and snowmelt water. Concentration versus discharge diagrams identified the dilution of weathering ions during melt, while the ratio of potassium to calcium in streamwater suggests early contributions of pre-event water to discharge. Results from this research support previous work that pre-event water dominates freshet, yet the role of deeper groundwater is highlighted as an important contribution.

**Key words** | hydrochemistry, isotopes, runoff, snowmelt, subarctic water balance

Jessica L. Boucher

Sean K. Carey (corresponding author)  
Department of Geography and Environmental  
Studies,  
Carleton University,  
Ottawa, Ontario,  
Canada K1S 5B6  
Tel.: +1 613 520 2600  
Fax: +1 613 520 4301  
E-mail: sean\_carey@carleton.ca

### INTRODUCTION

The processes and mechanisms that control runoff generation in northern environments where snowmelt, permafrost and frozen ground predominate have undergone considerable study in the discontinuous permafrost regions of northwestern North America (Dingman 1971; Santeford 1979; Slaughter *et al.* 1985; MacLean *et al.* 1999; Carey & Woo 2001; Carey & Quinton 2004, 2005; Petrone *et al.* 2006). In this environment, snowmelt is the dominant hydrological event, resulting in the bulk of the annual water delivery to the stream in a few short weeks. Streamflow hydrochemistry is strongly altered during this period (MacLean *et al.* 1999; Carey & Quinton 2004; Petrone *et al.* 2006) as near-surface runoff pathways predominate.

Prior to melt, dissolved ion concentrations associated with mineral weathering are high, reflecting deeper subsurface pathways sustaining baseflow, whereas nutrients and organic material that indicate near-surface runoff are largely absent. During melt, permafrost and frozen ground restrict deeper drainage, enhancing near-surface water tables through widely present organic horizons (Slaughter & Kane 1979; Carey & Woo 2001; Carey & Quinton 2004), enriching waters with nutrients, biologically active ions and dissolved organic carbon (DOC) (Carey 2003). Throughout the year, catchments and slopes with increased permafrost have greater DOC and nutrient concentrations and lower ionic strength due to near-surface pathways. Changing

doi: 10.2166/nh.2010.146

subsurface pathways in response to climate warming and its effect on DOC have been reported by *Striegl et al. (2005)*.

There has been an increase in the application of isotopic methods to determine source waters and to improve conceptual models of runoff generation at the hillslope scale in permafrost environments. Pre-event water dominates summer streamflow response in regions with permafrost, yet there is contrary evidence as to whether snowmelt (*Cooper et al. 1991, 1993; McNamara et al. 1997*) or groundwater supplies the bulk of the streamflow during freshet (*Obradovic & Sklash 1986; Gibson et al. 1993; Metcalfe & Buttle 2001; Carey & Quinton 2004*). Reasons for discrepancies point to the methods of event-water collection (cores vs. meltwater) and the large heterogeneity in hydrological processes, storage capacity of the soil and the relative permeability/impermeability of soils during freshet.

Our conceptual models of runoff generation in the subarctic are largely based on a few small headwater catchments (*Dingman 1971; Chacho & Bredhauer 1983; Slaughter et al. 1983; Carey & Quinton 2004, 2005; Petrone et al. 2006*) or hillslope/plot studies (*Carey & Woo 2001; Quinton et al. 2005, 2009*). There have been few reported studies combining stable isotopes (which do not participate in chemical reactions and provide information on water sources) and dissolved solutes (that do participate in reactions and provide information on flow pathways). This information is important as it provides an improved and refined understanding of runoff processes in this environment. Coupling of the water balance to runoff response is critical, as heterogeneity in process response is extremely high in alpine subarctic environments

(*Carey & Woo 1998*) and accurate determination of the volume of water infiltrating and reaching the stream will help constrain estimates of source water contributions.

The objectives of this research are to: (i) determine the water balance components during freshet and (ii) couple water balance information with stable isotope and hydrochemical information to provide an enhanced understanding of runoff sources and pathways during the critical snowmelt period. This research was conducted within Granger Basin (GB), a 7.6 km<sup>2</sup> headwater within the Wolf Creek Research Basin, Yukon Territory, which has been the subject of considerable process-based hydrological research. It is unique in that it is the first study to combine isotopic and hydrochemical analysis to evaluate snowmelt runoff in this basin.

## METHODS

### Site description

Granger Basin (60°32'N, 135°18'W) drains an area of 7.6 km<sup>2</sup> and ranges in elevation from 1,310–2,250 m (*Figure 1*) and is located within the Wolf Creek Research Basin, a long-term watershed research facility. The climate is continental subarctic, with mean annual precipitation 300–400 mm/yr with ~40% falling as snow. Mean annual temperature is –3°C with January and July temperatures of –17.7°C and +14.1°C (1971–2000).

GB has a geological composition that is primarily sedimentary, consisting of sandstone, siltstone, limestone and conglomerate, overlain by till ranging in thickness

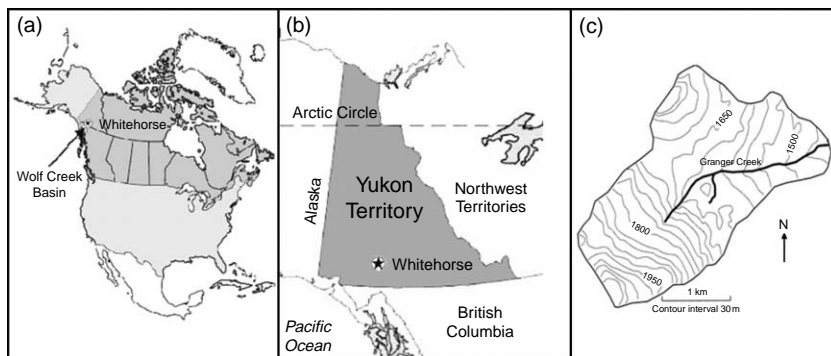


**Figure 1** | Location of Granger Basin within Canada.

from centimeters to 10 m (Mougout & Smith 1994). Atop the till, soils are capped with a surface organic layer at lower elevations ranging from 0.05–0.3 m. Permafrost underlies much of the catchment, particularly north-facing slopes and upper areas of the basin. Lewkowitz & Ednie (2004) suggest that 70–80% of GB is underlain with permafrost. Only a few scattered white spruce occur at lower elevations as GB is above the tree line. Vegetation consists of assorted willow shrubs at lower elevations with dwarf birch and tundra at higher elevations.

### Field methods

The study period was 10 April to 8 July 2008. Discharge was measured at the GB outlet using a well-established stage-discharge relation for open water conditions and salt dilution when snow and ice covered the channel. Continuous measurements of water quality parameters (specific conductance (SpC), pH, water temperature) were monitored using a Hydroloab 4a Datasonde.

A total of 185 water samples (122 stream, 37 snow and 26 ice) were collected by automated water samplers (ISCO) or grab sampling. Snowmelt water was collected using three snowmelt lysimeters (50 cm<sup>2</sup>) distributed throughout the catchment. Meltwater from the lysimeters was collected from sealed containers approximately every three days. Samples were stored in 60 mL air-tight bottles with minimal headspace. Eight snow transects were maintained throughout the study period to establish basin-wide snow water equivalent (SWE). Snow depth was measured along the transects (>40 points) using a Mount Rose snow sampler with density measurements every five points. Soil water and shallow groundwater samples collected in 2006 were used to estimate an average soil water hydrochemical and isotopic signature and were collected from suction lysimeters and shallow wells within GB. A full meteorological station existed within GB, measuring net and short-wave radiation, air temperature, humidity and wind speed, among other variables.

### Laboratory methods

Water samples were analyzed for isotopes of hydrogen (<sup>2</sup>H) and oxygen (<sup>18</sup>O) at the GG Hatch Stable Isotope

Laboratory at the University of Ottawa using a Finnigan MAT Delta plus XP + Gasbench isotope ratio mass spectrometer. The analytical precision for the <sup>2</sup>H and <sup>18</sup>O analysis was ± 1.5‰ and ± 0.10‰, respectively. All water samples were analyzed for major cations and anions using a DIONEX LC25 chromatography oven and CD20 conductivity detector in the Water Chemistry Laboratory at the University of Toronto. Anions evaluated are: chloride (Cl<sup>-</sup>), bromide (Br<sup>-</sup>), nitrate (NO<sub>3</sub><sup>-</sup>), phosphate (PO<sub>4</sub><sup>3-</sup>) and sulfate (SO<sub>4</sub><sup>2-</sup>). The cations evaluated include: sodium (Na<sup>+</sup>), ammonium (NH<sub>4</sub><sup>+</sup>), potassium (K<sup>+</sup>), magnesium (Mg<sup>2+</sup>) and calcium (Ca<sup>2+</sup>). The analytical detection limit for both anions and cations was ± 0.04 ppm.

### Hydrograph separation

Two-component hydrograph separations have been widely used to establish the sources of streamwater during snowmelt, and are based on the steady state mass balance equations for water and a conservative tracer (Sklash & Farvolden 1979):

$$Q_T = Q_p + Q_e \quad (1)$$

$$c_T^t Q_T = c_p^t Q_p + c_e^t Q_e \quad (2)$$

where  $Q_T$  is the total runoff,  $Q_p$  and  $Q_e$  are the pre-event and event runoff components, and  $c_p^t, c_e^t$  are the respective pre-event and event concentrations of the observed tracer  $t$ . The nature of this technique requires that (1) significant differences exist in the tracer concentrations of the components, (2) tracer concentrations of the individual components  $c_p^t, c_e^t$  are constant in space and time (or variations can be accounted for), (3) additional component contributions are negligible or the tracer concentrations must be similar to that of another component, (4) the tracers mix conservatively and (5) tracer concentrations of the components are not collinear (Hoeg *et al.* 2000). In this study,  $\delta^{18}\text{O}$  and  $\delta^2\text{H}$  were used for hydrograph separation due to their widespread application during snowmelt due to the depleted signature of meltwater that typically provides large differences between event and pre-event water (Rodhe 1981).

To estimate uncertainty associated with pre-event water, event water and streamwater values, it is necessary

to determine the systematic and analytical errors of the tracer signatures. The Gaussian standard error propagation technique as outlined by [Genereux \(1998\)](#) was applied:

$$W_{fp} = \sqrt{\left[ \frac{c_e - c_T}{(c_p - c_e)^2 W_{c_p}} \right]^2 + \left[ \frac{c_T - c_p}{(c_p - c_T)^2 W_{c_e}} \right]^2 + \left[ \frac{1}{(c_p - c_e)} W_{c_T} \right]^2} \quad (3)$$

where  $W$  is uncertainty,  $c$  is the tracer concentration,  $f$  is the fraction of total discharge and the subscripts p, e and T refer to the pre-event, event and streamwater components, respectively.

## RESULTS

### Snowmelt

Basin-average SWE on 21 April was 152 mm, although there was considerable variability based on slope, aspect and elevation ([Figure 2\(a\)](#)). Snowmelt declined at a slow yet steady rate at the beginning of the study period, with a few small snowfall events increasing the SWE. As temperatures warmed, all transects experienced enhanced melt between 20 May and 4 June when approximately 70% of all melt occurred. This corresponded to the period of increased

discharge and spring freshet. After 6 June, temperatures cooled and SWE did not decline again until 14 June when warmer temperatures melted most of the remaining snow. To highlight the variability in snowmelt patterns, the first transect to reach 0 SWE occurred on 29 May, compared with 7 July for the last.

### Discharge

Discharge measurements began on 11 April prior to the onset of melt and continued throughout the study period ([Figure 2\(b\)](#)). Prior to melt, baseflow values were  $\sim 0.01 \text{ m}^3 \text{ s}^{-1}$ . Despite a few small increases around 10 May as melt began, streamflow did not notably increase until 18 May when values rose to  $> 0.2 \text{ m}^3 \text{ s}^{-1}$  and then on 23 May rose rapidly to  $> 1 \text{ m}^3 \text{ s}^{-1}$ . The high-flow period occurred between 23 and 28 May during peak melt, with a maximum discharge of  $1.75 \text{ m}^3 \text{ s}^{-1}$  for the study period. Following 28 May, flows declined relatively quickly until 11 June due to cooling temperatures that reduced snowmelt inputs ([Figure 2\(b\)](#)). Between 11 and 21 June, warm temperatures, snowmelt and rainfall combined to increase discharge. By 19 June, snowmelt was near-complete, and streamflow declined to values between  $0.1$  and  $0.2 \text{ m}^3 \text{ s}^{-1}$  with intermittent variation resulting from rainfall events.

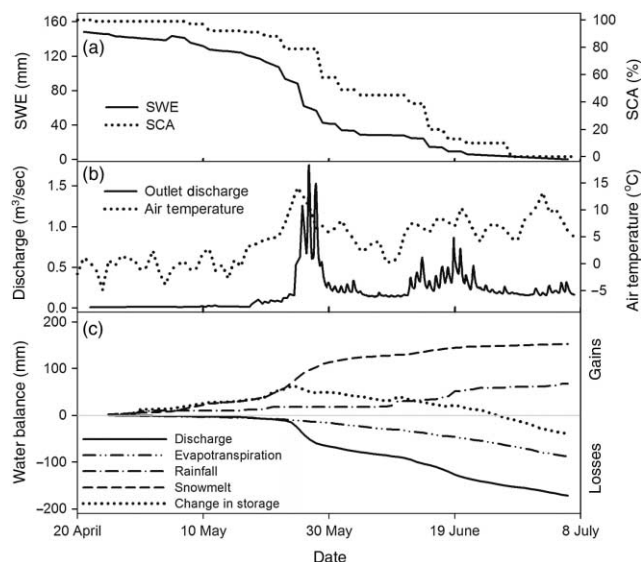


**Figure 2** | Time series of (a) Snow Water Equivalent (SWE) and Snow-Covered Area (SCA), (b) discharge and air temperature, and (c) cumulative water balance components.

### Water balance

The water balance for the snowmelt period was defined as

$$R + M - Q - E = \Delta S \quad (4)$$

where  $R$  is rainfall,  $M$  is water released from the snowpack,  $Q$  is discharge,  $E$  is evaporation and  $\Delta S$  is the change in all forms of storage within the basin. All values are determined in mm of liquid water. Discharge was measured directly; rainfall from a tipping-bucket gauge and  $M$  is taken as the daily sum of the SWE decline. Evaporation from bare ground was determined using the Priestley–Taylor method ([Priestley & Taylor 1972](#)) using  $\alpha = 1.26$  based on values used previously in this basin ([McCartney et al. 2006](#)). For snow, an evaporation (sublimation) value of  $0.2 \text{ mm/day}$  ([Pomeroy et al. 2003](#)) was applied to snow-covered areas. Daily evaporation was calculated as the weighted average

**Table 1** | Granger Basin outlet water balance components and runoff ratio. Period is 10 April–8 July 2008

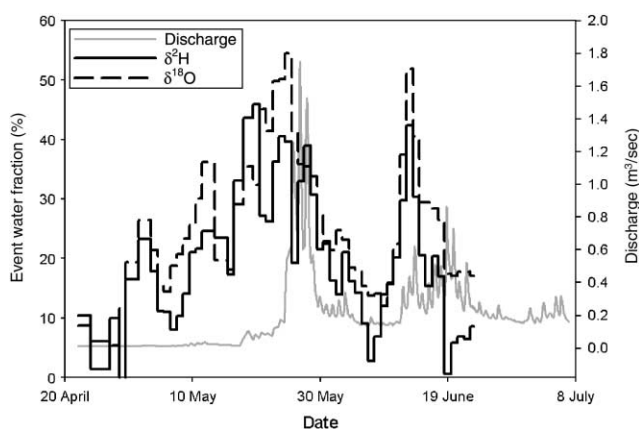
SWE (mm)	Rainfall (mm)	Evaporation (mm)	Discharge (mm)	Change in storage (mm)	Runoff ratio
152	68	88	173	−41	0.79

of snow-free and snow-covered areas using the two methods above.

Cumulative daily water balances during the study period show that snowmelt is the largest source of water to the system with discharge the largest loss (Figure 2(c)). GB gained water, increasing storage, during the initial phase of the study, as snowmelt gains were not offset by losses from  $Q$  or  $E$ . By 26 May, losses began to exceed gains and storage began to decline. At the end of the study period, there was  $\sim 41$  mm less water in GB than at the onset. Water balance components, along with the runoff ratio  $((P + M)/Q)$ , are shown in Table 1.

### Hydrograph separation

Two-component hydrograph separations were performed for  $\delta^{18}\text{O}$  and  $\delta^2\text{H}$  tracers (Figure 3). Event-water isotope values were calculated using volume-weighted averaging of the samples collected in the three snowmelt lysimeters. Pre-melt baseflow samples were used to estimate pre-event values, and the volume-weighted value of water from snowmelt lysimeters was used to estimate the event-water value.

**Figure 3** | Two-component hydrograph separations for  $\delta^{18}\text{O}$  and  $\delta^2\text{H}$ .

Hydrograph separation using  $\delta^2\text{H}$  estimated that event water accounted for 23% (40 mm) of discharge and pre-event water contributed 77% (133 mm) throughout the study period. Conversely, using  $\delta^{18}\text{O}$ , pre-event water contributed 32% (55 mm) of discharge with pre-event contributing 68% (118 mm). The relative fractions of event and pre-event water contributions varied throughout the study period. At the onset of the study, both  $\delta^2\text{H}$  and  $\delta^{18}\text{O}$  demonstrate low event-water fractions, as would be expected from using baseflow as an end-member. Event-water contributions (based on both isotopes) rapidly increased to a maximum just prior to peak freshet. During the peak freshet period, between 25 and 30 May, both isotopes suggest approximately equal contributions of event and pre-event water. Following this, pre-event water was responsible for the majority of streamflow during the declining phase of flow. Event-water contributions increased once more during a high melt and rainfall event after 13 June.

The error associated with the hydrograph separations was evaluated using Equation (3). Pre-event, event and streamwater components and their respective analytical and measurement error are presented in Table 2. For pre-event water ( $c_p$ ), the uncertainty ( $W_{c_p}$ ) was calculated as the coefficient of variation of the pre-event baseflow values prior to snowmelt. The event water ( $c_e$ ) uncertainty ( $W_{c_e}$ ) was calculated as the coefficient of variation of the snowmelt water values. Streamwater uncertainty ( $W_{c_T}$ ) was estimated using the analytical error associated with

**Table 2** | Uncertainty for pre-event, event and streamwater components for both  $\delta^{18}\text{O}$  and  $\delta^2\text{H}$ 

Component		$\delta^{18}\text{O}$	$\delta^2\text{H}$
Pre-event	$c_p$ (‰)	−21.19	−165.32
	$W_{c_p}$ (%)	$\pm 1.3$	$\pm 1.0$
Event	$c_e$ (‰)	−24.18	−188.12
	$W_{c_e}$ (%)	$\pm 5.3$	$\pm 4.9$
Total stream	$c_T$ (‰)	Sample value	Sample value
	$W_{c_T}$ (%)	$\pm 0.7$	$\pm 1.1$ – $1.2$
Total average percent error (%)		$\pm 8.9$	$\pm 2.5$
Total percent error range (%)		$\pm 3.3$ – $33.1$	$\pm 0.2$ – $13.4$



each isotope. The estimated average daily percent error of pre-event water for  $\delta^{18}\text{O}$  was 8.9% and for  $\delta^2\text{H}$  was 2.5%. However, during certain periods of the separation, errors were large for  $\delta^2\text{H}$  as when streamflow values fell within the standard-error of the pre-event signature. On 26 April, 29 April, 7 June and 19 June the percent errors for  $\delta^2\text{H}$  stream values were 234.5, 1420.8, 60.5 and 1225.0%, respectively. If these large error values are included, the average error for  $\delta^2\text{H}$  is 56.8%, yet on a flow-weighted basis are still  $<6\%$ . Similar errors were not observed for  $\delta^{18}\text{O}$ .

### Isotope and hydrochemical response

The stable isotopes of water ( $\delta^{18}\text{O}$  and  $\delta^2\text{H}$ ) were measured daily at the outlet and when water was present in the snowmelt lysimeters (Figure 4).

The stream values of  $\delta^{18}\text{O}$  and  $\delta^2\text{H}$  behaved similarly, yet there were a few distinct differences (Figure 4).

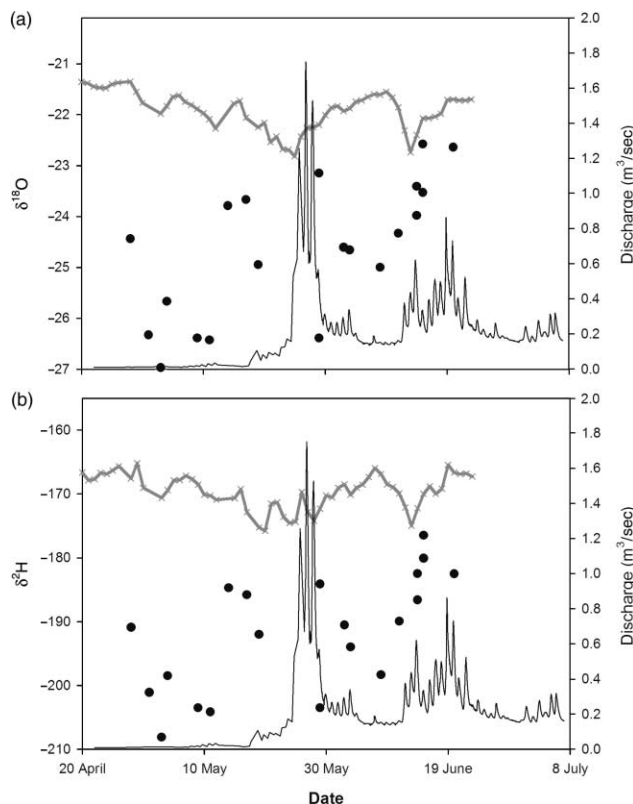


**Figure 4** | Time series of (a)  $\delta^{18}\text{O}$  and (b)  $\delta^2\text{H}$  observed at the outlet (dark grey symbols and line), and from snowmelt lysimeters (black circles). Solid black line is discharge at the basin outlet (right axis).

There were two prominent depletion episodes for both isotopes that occurred around the peak snowmelt period, 26 May, and the peak precipitation period, 19 June.  $\delta^{18}\text{O}$  was relatively enriched prior to snowmelt (20 April  $\delta^{18}\text{O} = -21.36\text{‰}$ ) and was most depleted during the peak snowmelt and streamflow period (25 May =  $-22.82\text{‰}$ ). A second depletion period occurs on 13 June ( $-22.74\text{‰}$ ), which coincided with the largest snowfall event of the study period.  $\delta^2\text{H}$  was also the most enriched prior to snowmelt (26 April =  $-165.64\text{‰}$ ) although it became most depleted slightly earlier than the peak snowmelt and peak streamflow period (20 May =  $-175.78\text{‰}$ ). A second depletion period occurred on 13 June ( $-174.98\text{‰}$ ), which also coincided with the largest snowfall event of the study period. These trends were observed at Location B, Location C and the outlet to varying degrees and are indicative of characteristically depleted snowmelt water reaching the stream.

Of the major anions and cations analyzed, sodium ( $\text{Na}^+$ ), potassium ( $\text{K}^+$ ), magnesium ( $\text{Mg}^{2+}$ ), calcium ( $\text{Ca}^{2+}$ ), chloride ( $\text{Cl}^-$ ), nitrate ( $\text{NO}_3^-$ ) and sulfate ( $\text{SO}_4^{2-}$ ) were above the detection limit. Both bromide ( $\text{Br}^-$ ) and ammonium ( $\text{NH}_4^+$ ) were below the detection limit. There are several distinct patterns: ions that dilute with increased flow ( $\text{Ca}^{2+}$ ,  $\text{Na}^+$ ,  $\text{Mg}^{2+}$ ,  $\text{SO}_4^{2-}$ ,  $\text{Na}^+$ ), those that tend to increase ( $\text{K}^+$ ) or show no general trend ( $\text{NO}_3^-$ ) (Figure 5).  $\text{Ca}^{2+}$ ,  $\text{Na}^+$ ,  $\text{Mg}^{2+}$  and  $\text{SO}_4^{2-}$  are all ions associated with mineral weathering and were at their peak concentrations prior to the onset of freshet. As snowmelt began in the basin, their concentrations began to gradually dilute, falling after 10 May and then reaching a local minima during peak

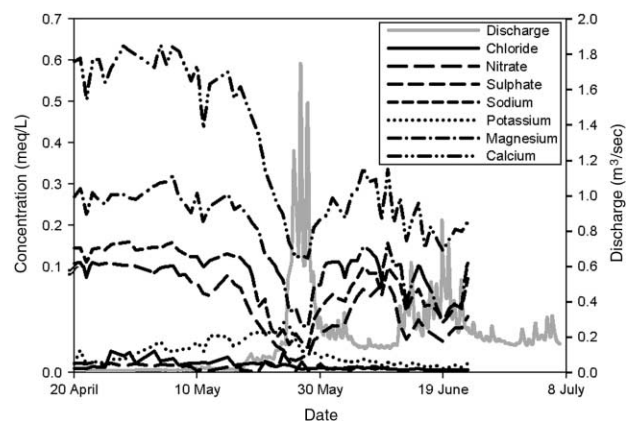


**Figure 5** | Time series of major ions and discharge.

freshet. Despite low concentrations during this time, the greatest mass flux of these ions occurred during peak flows. Following 30 May and the decline in flows, concentrations increased, only to once again decrease coinciding with the second high-flow event after 14 June. In contrast,  $K^+$  and

$NO_3^-$  showed weak trends, with a general increase in concentration with flows at the onset of freshet, with only small patterns thereafter.

Concentration–discharge relationships are an alternative method of exploring hydrochemical response, and have

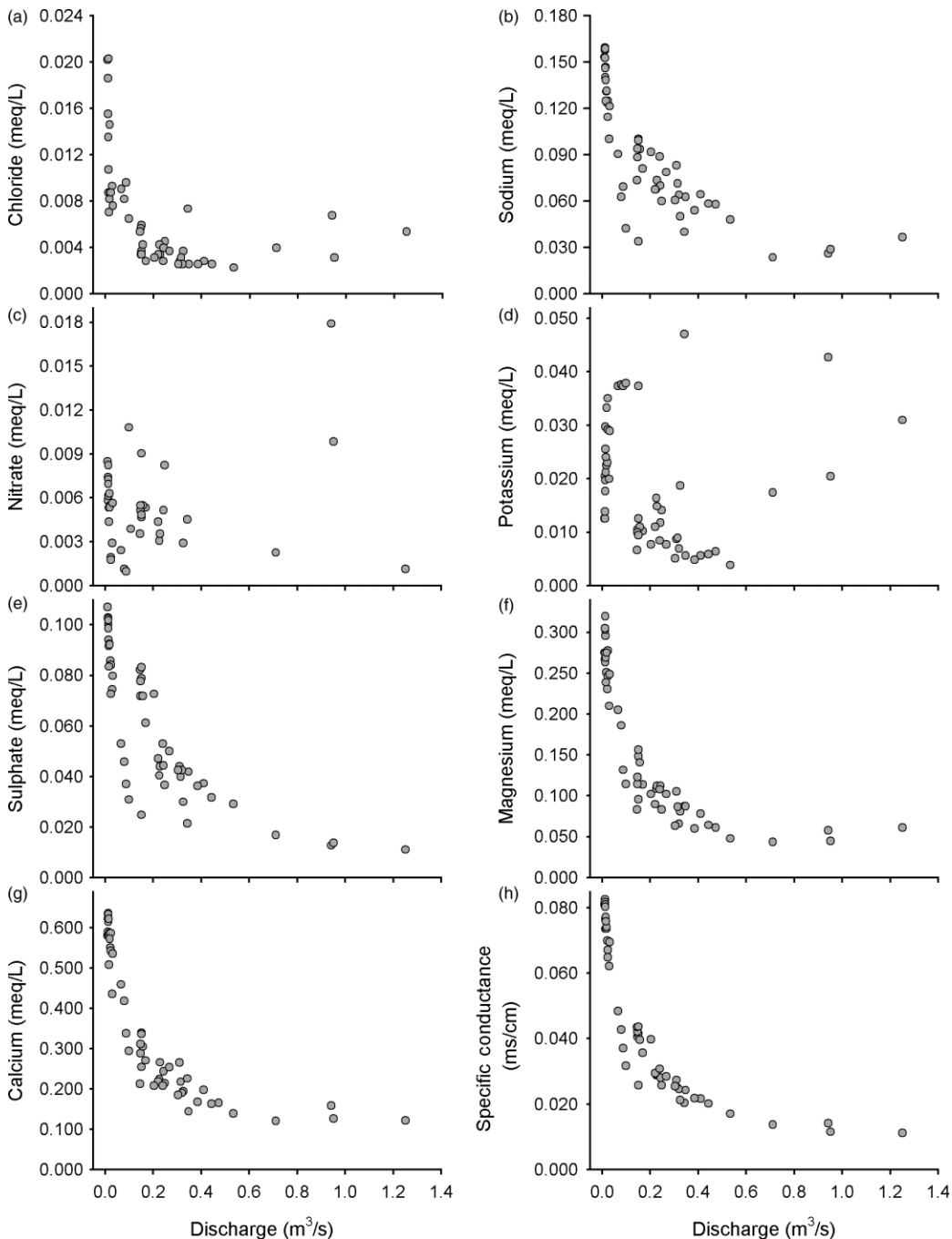


**Figure 6** | Concentration versus discharge plots for all ions and specific conductance.

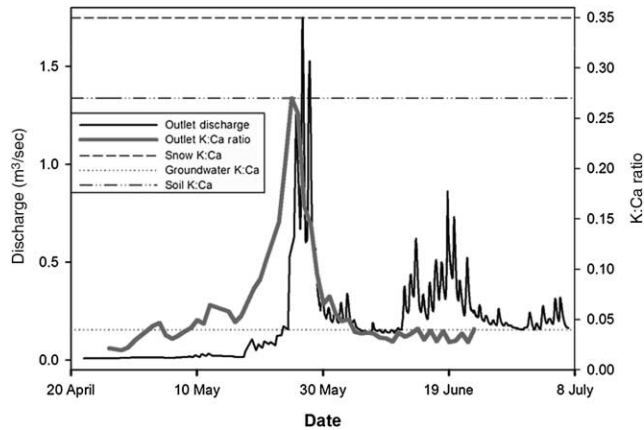


**Figure 7** | Time series of K:Ca molar ratio and hydrograph. Groundwater and soil water K:Ca ratios are also shown as horizontal lines.

often been used to infer catchment behavior (e.g. Godsey *et al.* 2009). Plots of ions versus instantaneous discharge (Figure 6) revealed that most ions and specific conductance had an inverse concentration–discharge relationship. For the weathering cations ( $Mg^{2+}$ ,  $Ca^{2+}$ ) these relationships are highly log-linear; suggesting dilution of water during freshet. In contrast, ions that are more biologically active ( $K^+$ ,  $NO_3^-$ ) showed poor relations with discharge, and changes in their concentration were more indicative with flow from near-surface organic horizons.

Aqueous molar solute ratios are often used to evaluate sources of water, reflecting changes with depth in the soil

profile of biologically active and inactive ions in solution. The ratio of  $K^+ : Ca^{2+}$  (Figure 7) represents the relative importance of near-surface water in the organic layer (high  $K^+$  concentrations) to that of deeper subsurface flow in the mineral horizons (high  $Ca^{2+}$  concentrations). Large ratios denote fast or surface pathways and small ratios slower subsurface pathways (Elsenbeer *et al.* 1995). The  $K^+ : Ca^{2+}$  ratio was initially low with values near that obtained from groundwater samples. As melt progressed, the ratio increased towards that of soil water, several days in advance of peak freshet. Following this, values quickly declined to pre-event ratios.

A total of 36 end-member mixing diagrams (using soil, snow and deep groundwater as the end-members) were conducted for all possible combinations of the seven major ions as well as  $\delta^{18}O$  and  $\delta^2H$  in order to further evaluate sources of streamflow water. Of these, the most appropriate were the combinations of chloride ( $Cl^-$ ),  $\delta^{18}O$  and  $\delta^2H$  (Figure 8), which understandably showed similar trends. For both the  $Cl^-$  vs  $\delta^{18}O$  and  $Cl^-$  vs  $\delta^2H$  diagrams, pre-melt streamflow chemistry began at the groundwater end-member. Streamwater then deflected towards the soil-water end member and then moved towards the snowmelt end-member. Towards the end of the study period, stream values returned towards the groundwater end-member, yet were no longer bound by the three proposed end-members. A likely explanation for this is the rainfall event on 19 June,

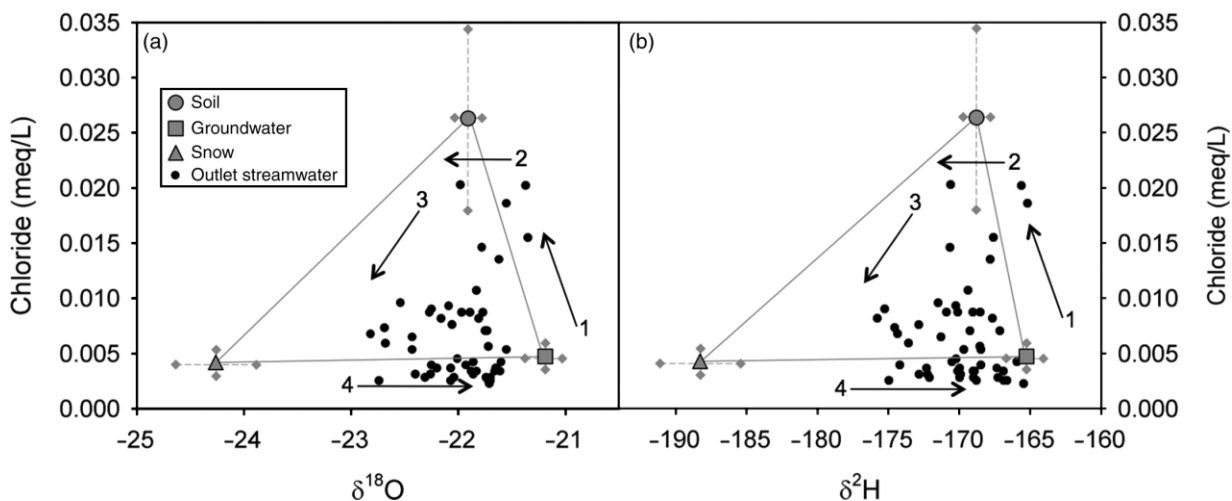


**Figure 8** | Snow, soil and groundwater end-member mixing diagrams for (a) chloride vs.  $\delta^{18}O$  and (b) chloride vs.  $\delta^2H$  ( $\pm$  standard error). Arrows indicate the direction of streamflow evolution (1 being the start and 4 being the end).



which was not sampled. Based on previous rainwater samples, precipitation was likely enriched compared with groundwater at this time, providing an explanation as to why the existing end-members no longer bound streamflow concentrations.

## DISCUSSION

Snowmelt is the dominant hydrochemical and hydrometric event in subarctic catchments, transferring much of the annual precipitation to the stream over approximately one month and strongly impacting the hydrochemistry of the stream. During melt, much of the catchment soils are saturated, particularly permafrost-underlain areas, and near-surface flow pathways convey water rapidly to the stream. The pathways that runoff takes are strongly controlled by the position of the water table as positive feedback occurs where faster runoff rates (and more runoff from precipitation events) occurs when the water table is near the surface (Carey & Woo 2001; Quinton *et al.* 2009). The source of this water, whether it resides within the catchment prior to inputs (pre-event or old water), or water precipitated on the catchment transferred directly to the stream (event or new water), is the subject of much debate. In permafrost settings, it is typically thought that low storage capacity and high runoff ratios, particularly during melt, would result in new water dominating the hydrograph.

Results from this study suggest that, for Granger Basin, an alpine discontinuous permafrost catchment, freshet is largely derived from water that existed in the soil prior to melt. This result (23% for  $\delta^2\text{H}$  and 32% for  $\delta^{18}\text{O}$ ) is in the low range of results reported for permafrost-underlain soils, which typically have larger new-water contributions (Obradovic & Sklash 1986; Cooper *et al.* 1991; Gibson *et al.* 1993; McNamara *et al.* 1997; Metcalfe & Buttle 2001). For GB, two-component hydrograph separations by Carey *et al.* (2009) indicate that, for four years, event-water contribution varied between 10 and 26%. Inter-annual differences in event water may in part be explained by differences in the freshet water balance. As a means of comparison, four years of water balance and two-component hydrographs for GB are presented in Table 3. Water balance components and runoff ratios were re-calculated for the 20 April to 1 July

**Table 3** | Granger Basin water balance components, melt period air temperature and event-water contributions using  $\delta^{18}\text{O}$  for four years. Period is 20 April–1 July

Year	2002	2003	2006	2008
Runoff (mm)	112	62	118	147
SWE (mm)	213	190	160	152
Precipitation (mm)	24	27	76	68
SWE + precipitation (mm)	237	217	236	220
Runoff ratio	0.47	0.29	0.50	0.67
Previous August–October Rainfall (mm)	69	74	80.3	109
April–June air temp (°C)	4.9	6.2	6.6	6.4
Event-water contribution	22	10	26	32
Maximum event water contribution	0.47	0.29	0.50	0.55

period and two-component hydrograph separations for  $\delta^{18}\text{O}$  only. Note that this period is slightly shorter than reported in Table 1. Considering that there are large differences in the timing and magnitude of melt, the water balance components and the discharge, there is surprisingly little variability in event-water contributions among years 2002, 2006 and 2008. For these three years, runoff ratios were high and there is evidence suggesting that these are related to antecedent wetness in the catchment reflected by the previous fall precipitation. In addition, they had greater total precipitation during the melt period and a single melt event, whereas 2003 was a slow melt year characterized by multiple melt events, providing increased infiltration opportunity time, lower runoff ratios and lower event-water contributions (~10%).

There is a large degree of uncertainty in the two-component hydrograph separations presented. While the Gaussian error propagation method of Generaux (1998) provides error estimates, actual errors are likely higher as the sampling strategy for measuring meltwater inputs is limited in its spatial scale. Field data from GB (not shown) suggests that the spatial variability of the meltwater isotopic signature is large, and characterizing event water from one site may not adequately characterize the input chemical signature. In addition, the method for determining  $c_e$  assumes no catchment storage and that all meltwater is instantaneously routed to the streams. Other methods such as those presented by Laudon *et al.* (2002) may be more appropriate for characterizing event-water signatures, yet

require detailed information on basin storage, which is difficult to determine at larger scales.

While this study and others confirm that old water residing within GB dominates the freshet hydrograph, it is unclear as to how this old water actually reaches the stream as stable isotopes do not provide information on runoff pathways. Runoff processes have previously been studied in GB (Carey & Quinton 2004, 2005; McCartney *et al.* 2006; Quinton *et al.* 2009) and hydrometric evidence suggests that near-surface runoff, primarily flow through organic layers, controls the rate and timing of the snowmelt hydrograph. In frozen soils, it is uncertain how old water that is largely immobile can be displaced by new event water from snowmelt, which is used in part to describe rapid old-water signatures in more temperate environments (Laudon *et al.* 2004).

Runoff chemistry provides a means to assess the pathways of water flow through the catchment. Here, focus will be restricted to the weathering ions  $\text{Ca}^{2+}$  and  $\text{Mg}^{2+}$  that have high concentrations in deeper groundwater sources, and the biologically active ion  $\text{K}^+$  that has greater abundance in surface-organic soil water. Previous conceptual models of runoff generation in GB and permafrost-underlain catchments suggest meltwater infiltrates and percolates from the snowpack into frozen unsaturated organic soils. These organic soils saturate from the organic/mineral interface to the surface, generating runoff through rapid near-surface pathways. Runoff generation is thought to be largely confined to permafrost-underlain slopes, as many areas of the catchment are snow-free before freshet begins (Carey & Quinton 2004). Hydrochemical data indicates that, prior to freshet, groundwater dominates baseflow. As streamflow begins to increase,  $\text{Ca}^{2+}$  and  $\text{Mg}^{2+}$  decline, whereas  $\text{K}^+$  increases. The molar ratio of  $\text{K}^+:\text{Ca}^{2+}$ , which increases with near-surface flow, rises prior to peak freshet as near-surface organic soils saturate and begin to generate runoff. During peak freshet,  $\text{K}^+:\text{Ca}^{2+}$  declines as either snowmelt water directly contributes and/or soil water K concentration declines. The pattern of  $\text{K}^+:\text{Ca}^{2+}$  is similar to that of DOC observed in GB (Carey 2003), which also peaks prior to freshet and rapidly declines as labile carbon is flushed from soils. Mixing diagrams with  $\text{Cl}^-$  and the stable isotopes of water corroborate hydrochemical data in that, at the onset of the study period,

groundwater predominates, followed by organic soil water, snowmelt water and then back towards groundwater. While end-members do not perfectly bind the mixing diagrams, the general pattern of runoff pathways is provided.

Unlike previous conceptual models of runoff generation for GB, hydrochemical data suggests a greater source of deep subsurface groundwater in providing water for freshet. Whereas Carey & Woo (2001) and Carey & Quinton (2004) largely dismiss the role of deeper groundwater as a source of water during freshet, hydrochemical data suggests that it is a major contributing factor. Our understanding of surface-groundwater interactions in alpine and permafrost watersheds is poor, mostly due to the lack of monitoring infrastructure (such as groundwater wells) and high spatial variability. Deep subsurface flow helps reconcile old-water contributions from stable isotopes with stream hydrochemistry, but it is still unclear how this water reaches the stream in such a rapid manner when soils are largely frozen and hydrological connections between snowmelt and deep subsurface water have not been directly observed.

## CONCLUSIONS

Hydrometric, isotopic and hydrochemical methods were utilized within Granger Basin, a 7.6 km<sup>2</sup> discontinuous permafrost watershed, to examine runoff components during the freshet period. It builds on previous work (Carey & Quinton 2004; McCartney *et al.* 2006) in that it utilized both chemical and hydrometric sampling to evaluate runoff components. Water balance data indicated that almost 80% of the melt and rainwater provided to the catchment during the 10 April–8 July 2008 study period was transmitted to the stream as runoff. The runoff ratio was greater than other years, and can in part be explained by wet antecedent soil conditions and a relatively rapid single melt event. Pre-event water accounted for ~27% of total streamflow based on an average of the  $\delta^2\text{H}$  and  $\delta^{18}\text{O}$  two-component hydrograph separations. Like the runoff ratio, this was high compared with other years where event water ranged from 10–26%. Hence, the vast majority of water in the stream during melt existed within the catchment over winter and was displaced during the freshet period. The pathways of this water were explored using a combination

of hydrochemical techniques. Solute time series, solute ratios and end-member mixing diagrams indicate that, prior to melt, deep subsurface pathways are responsible for streamflow. As melt occurs, organic soils begin to saturate and near-surface runoff pathways become active. Following this, saturated soils allow a larger conveyance of meltwater directly to the stream, resulting in high event-water contributions during freshet and lower concentrations of ions associated with organic layers ( $K^+$ ). As the melt period ends, the catchment dries and groundwater is again responsible for the majority of streamflow. However, during this entire sequence, deep subsurface groundwater is a major contributor to discharge during all periods.

Whereas previous research has identified permafrost slopes as the linchpin of runoff generation, hydrochemical evidence suggests that deeper groundwater sources play an important role in freshet streamflow. The nature of this surface-groundwater interaction, and how it varies within a basin, remains unclear and should be the focus of further integrated studies.

## ACKNOWLEDGEMENTS

This work is funded by research grants from NSERC and the CFCAS. The support of Glenn Ford and Ric Janowicz of the Water Resource Branch, Yukon Department of Environment, and the field assistance of Shawn MacDonald and Mike Treberg are gratefully acknowledged.

## REFERENCES

- Carey, S. K. 2003 Dissolved organic carbon fluxes in a discontinuous permafrost Subarctic alpine catchment. *Permafrost Periglacial Process*. **14**, 161–171.
- Carey, S. K. & Woo, M. K. 1998 Snowmelt hydrology of two subarctic slopes, southern Yukon, Canada. *Nord. Hydrol.* **29**, 331–346.
- Carey, S. K. & Woo, M. K. 2001 Spatial variability of hillslope water balance, Wolf Creek basin, subarctic Yukon. *Hydrol. Process.* **15**, 3113–3132.
- Carey, S. K. & Quinton, W. L. 2004 Evaluating snowmelt runoff generation in a discontinuous permafrost catchment using stable isotope, hydrochemical and hydrometric data. *Nord. Hydrol.* **35**, 309–324.
- Carey, S. K. & Quinton, W. L. 2005 Evaluating runoff generation during summer using hydrometric, stable isotope, and hydrochemical methods in a discontinuous permafrost alpine catchment. *Hydrol. Process.* **19**, 95–114.
- Carey, S. K., Boucher, J. L. & Duarte, C. M. 2009 A multi-year perspective on snowmelt runoff generation in an alpine subarctic catchment. In: *Proc. 17th International Northern Research Basin Symposium and Workshop, Canada*. York University, Toronto, pp. 77–86.
- Chacho, E. F. & Bredhauer, S. 1983 Runoff from a small sub-arctic watershed, Alaska. In: *Proc. Fourth International Conference on Permafrost*. National Academy Press, Washington, DC, pp. 115–120.
- Cooper, L. W., Olsen, C. R., Solomon, D. K., Larsen, I. L., Cook, R. B. & Grebmeier, J. M. 1991 Stable isotopes of oxygen and natural and fallout radionuclides used for tracing runoff during snowmelt in an arctic watershed. *Water Resour. Res.* **27**, 2171–2179.
- Cooper, L. W., Solis, C., Kane, D. L. & Hinzman, L. D. 1995 Application of oxygen-18 tracer techniques to Arctic hydrological processes. *Arct. Alp. Res.* **25**, 247–255.
- Dingman, S. L. 1971 *Hydrology of Glenn Creek Watershed, Tanana Basin, Central Alaska*. US Army Cold Region Research Engineering Laboratory Research Report 297, Hanover, NH.
- Elsenbeer, H., Lack, A. & Cassel, K. 1995 Chemical fingerprints of hydrological compartments and flow paths at La Cuenca, western Amazonia. *Water Resour. Res.* **31**, 3051–3058.
- Genereux, D. P. 1998 Quantifying uncertainty in tracer-based hydrograph separations. *Water Resour. Res.* **34**, 915–919.
- Gibson, J. J., Edwards, T. W. D. & Prowse, T. D. 1995 Runoff generation in a high boreal wetland in northern Canada. *Nord. Hydrol.* **24**, 213–224.
- Godsey, S. E., Kirchner, J. W. & Clow, D. W. 2009 Concentration-discharge relationships reflect chemostatic characteristics of US catchments. *Hydrol. Process.* **23**, 1844–1864.
- Hoeg, S., Uhlenbrook, S. & Leibundgut, C. 2000 Hydrograph separation in a mountainous catchment—combining hydrochemical and isotopic tracers. *Hydrol. Process.* **14**, 1199–1216.
- Laudon, H., Hemond, H. F., Krouse, R. & Bishop, K. H. 2002 Oxygen 18 fractionation during snowmelt: implications for spring flood hydrograph separation. *Water Resour. Res.* **38**, 1258.
- Laudon, H., Seibert, J., Kohler, S. & Bishop, K. 2004 Hydrological flow paths during snowmelt: congruence between hydrometric measurements and oxygen 18 in meltwater, soil water, and runoff. *Water Resour. Res.* **40**(W03102) (doi: 10.1029/2003WR002455).
- Lewkowicz, A. G. & Ednie, M. 2004 Probability mapping of mountain permafrost using the BTS method, Wolf Creek, Yukon Territory, Canada. *Permafrost Periglacial Process.* **15**, 67–80.
- MacLean, R., Oswood, M. W., Irons, J. G., III & McDowell, W. H. 1999 The effect of permafrost on stream biogeochemistry: a case study of two streams in the Alaskan (U.S.A.) taiga. *Biogeochemistry* **47**, 239–267.

- McCartney, S. E., Carey, S. K. & Pomeroy, J. W. 2006 Intra-basin variability of snowmelt water balance calculations in a subarctic catchment. *Hydrol. Process.* **20**, 1001–1016.
- McNamara, J. P., Kane, D. L. & Hinzman, L. D. 1997 Hydrograph separations in an Arctic watershed using mixing model and graphical techniques. *Water Resour. Res.* **33**, 1707–1719.
- Metcalfe, R. A. & Buttle, J. M. 2001 Soil partitioning and surface store controls on spring runoff from boreal forest peatland basin in north-central Manitoba, Canada. *Hydrol. Process.* **15**, 2305–2324.
- Mougout, C. M. & Smith, C. A. S. 1994 *Soil Survey of the Whitehorse Area* vol. 1. *Takhini Valley*. Research Branch, Agriculture and Agri-Food Canada, Whitehorse, 56.
- Obradovic, M. M. & Sklash, M. G. 1986 An isotopic and geochemical study of snowmelt runoff in a small arctic watershed. *Hydrol. Process.* **1**, 15–30.
- Petrone, K. C., Jones, J. B., Hinzman, L. D. & Boone, R. D. 2006 Seasonal export of carbon, nitrogen, and major solutes from Alaskan catchments with discontinuous permafrost. *J. Geophys. Res.* **111**, G02020.
- Pomeroy, J. W., Toth, B., Granger, R. J., Hedstrom, N. R. & Essery, R. L. H. 2003 Variation in surface energetics during snowmelt in a subarctic mountain catchment. *J. Hydrometeorol.* **4**, 702–719.
- Priestley, C. H. B. & Taylor, R. J. 1972 On the assessment of surface heat flux and evaporation using large scale parameters. *Mon. Weather Rev.* **100**, 81–92.
- Quinton, W. L., Shirazi, T., Carey, S. K. & Pomeroy, J. W. 2005 Soil water storage and active-layer development in a sub-alpine tundra hillslope, southern Yukon Territory, Canada. *Permafrost Periglacial Process.* **16**, 369–382.
- Quinton, W. L., Bemrose, R. K., Zhang, Y. & Carey, S. K. 2009 The influence of spatial variability in snowmelt and active layer thaw on hillslope drainage for an alpine tundra hillslope. *Hydrol. Process.* **23**, 2628–2639.
- Rodhe, A. 1981 Spring flood: meltwater or groundwater? *Nord. Hydrol.* **12**, 21–30.
- Santeford, H. S. 1979 Snow soil interactions in interior Alaska. In: *Proceedings of Modeling of Snow Cover Runoff*. Cold Regions Research and Engineering Laboratory, Hanover, NH, pp. 311–318.
- Sklash, M. G. & Farvolden, R. N. 1979 The role of groundwater in storm runoff. *J. Hydrol.* **43**, 45–66.
- Slaughter, C. W., Hilgert, J. W. & Culp, E. H. 1983 Summer streamflow and sediment yield from discontinuous-permafrost headwaters catchments. In: *Proc. Fourth International Conference on Permafrost*. National Academy Press, Washington, DC, pp. 1172–1177.
- Slaughter, C. W. & Kane, D. L. 1979 Hydrologic role of shallow organic soils in cold climates. In: *Proceedings of the Canadian Hydrology Symposium: 79–Cold Climate Hydrology*, Associate Committee on Hydrology, National Research Council, Vancouver, pp. 380–389.
- Striegl, R. G., Aiken, G. R., Dornblaser, M. M., Raymond, P. A. & Wickland, K. P. 2005 A decrease in discharge-normalized DOC export by the Yukon River during summer through autumn. *Geophys. Res. Lett.* **32**, L21413.

First received 4 November 2009; accepted in revised form 7 June 2010. Available online September 2010